The Science of Nature, Volume 113, Issue 3, June 2026, Article number 52
DOI: 10.1007/s00114-026-02103-5

Cuticular Hydrocarbons as Biomarkers of Developmental Stages in *Thanatophilus sinuatus* (Fabricius, 1775) (Coleoptera: Staphylinidae): Evidence from GC–MS and Random Forest Modeling

[1, 5] SWAIMA SHARIF, [2] PAVEL JAKUBEC, [3] HANNAH MOORE, [4] ROBERT CODY, [1]JENS AMENDT, [5, *]AYESHA QAMAR

[1] SWAIMA SHARIF

Institute of Legal Medicine, Forensic Biology
University Hospital, Goethe University, Frankfurt am Main, Germany
Email: swaimasharif@gmail.com

[2] PAVEL JAKUBEC

Faculty of Environmental Sciences, Czech University of Life Sciences Prague, Kamýcká 129, Praha – Suchdol, 165 00, Czech Republic (or Czechia).

Email: jakubecp@fzp.czu.cz

[3] HANNAH E MOORE

Cranfield Forensic Institute, Cranfield University, Defence Academy of the United Kingdom, Shrivenham, Wiltshire SN6 8LA, UK

Email: H.E.Moore@cranfield.ac.uk

[4] ROBERT B CODY

JEOL USA Inc, Peabody, MA, USA

Email: cody@jeol.com

[1] JENS AMENDT
Institute of Legal Medicine, Forensic Biology
University Hospital, Goethe University, Frankfurt am Main, Germany
Email: amendt@em.uni-frankfurt.de
ORCID: 0000-0001-8050-3211

[5, *] AYESHA QAMAR
Section of Entomology; Department of Zoology
Aligarh Muslim University, Aligarh, U.P., India, 202002
Email: ayesha.zoology@gmail.com
* Corresponding Author: Ayesha Qamar
ORCID: 0000-0008-2285-8254

Published by Springer. This is the Author Accepted Manuscript issued with: Creative Commons Attribution License (CC:BY 4.0).
The final published version (version of record) is available online at DOI:10.1007/s00114-026-02103-5. Please refer to any applicable publisher terms of use.

ABSTRACT

The analysis of cuticular hydrocarbon (CHC) profiles can provide valuable insights into species identification, immature development and adult ageing, sexual communication, reproductive functions, and other physiological processes of insects. This study investigated the CHC profiles across the life stages of *Thanatophilus sinuatus* (Fabricius, 1775), a carrion beetle species commonly associated with decomposing tissues, including human remains. We examined the first, second, and third larval instars, the pupa, and the adult male and female using gas chromatography–mass spectrometry. A total of 56 CHCs were identified, including *n*-alkanes, branched alkanes, and alkenes. Branched alkanes were dominant throughout development, while significant compositional differences were observed among stages. Certain compounds showed consistent proportions across development, suggesting roles in physiological or behavioral processes. Gender-specific differences were also evident, with some CHCs detected exclusively in males or females, potentially linked to sexual communication and reproductive functions. Principal component analysis revealed distinct clustering of developmental stages, and Random Forest classification with out-of-bag validation confirmed high predictive accuracy of CHC profiles for developmental stage identification. These findings highlight the potential of CHC profiling, combined with machine learning approaches, as a valuable tool, particularly useful in situations where specimens of *T. sinuatus* or other related species are damaged, incomplete, or present only as chemical residues, rather than when intact larvae are available. CHC profiling offers a complementary method for cases where diagnostic characters are missing or obscured.

Key Words- Cuticular hydrocarbons, Staphylinidae, life stages, *n*-alkanes, branched alkanes, confusion matrix.

INTRODUCTION

Forensic entomology has historically prioritized Diptera, especially blowflies (Calliphoridae), due to their rapid colonization of dead bodies and the subsequent, relatively predictable development. However, beetles such as those from the genera *Thanatophilus* and *Necrodes* have been underutilized in forensic applications, despite their presence during later decomposition stages and

potential to refine post-mortem interval (PMI) estimations (Matuszewski et al. 2008; Midgley and Villet 2009; Dekeirsschieter et al. 2011; Ridgeway et al. 2014).

Here, *Thanatophilus sinuatus* (Fabricius, 1775) is of particular forensic relevance as it colonizes cadavers earlier than most other beetles and occurs across various habitats in the Palaearctic (Ratcliffe and Luedtke 1969; Frątczak-Łagiewska and Matuszewski 2018; Jakubec et al. 2019). Accurate estimation of the post-mortem interval (PMI) and, in particular, the minimum PMI (minPMI) that can be inferred from insect development often depends on identifying and aging the oldest insect stage present (Amendt et al. 2011). Traditional approaches rely heavily on morphological characteristics and species-specific developmental models, especially thermal summation models, which require precise species and instar identification (Ridgeway et al. 2014).

However, morphological species identification of larval stages within *Thanatophilus* is notoriously difficult. The three larval instars of *T. sinuatus* can generally be distinguished using size and head-capsule characters (Jakubec et al. 2019). The difficulty reported in the literature refers mainly to separating larvae of *T. sinuatus* from those of the closely related *T. rugosus*, which often occur together on remains and are morphologically indistinguishable until the third instar (Frątczak and Matuszewski 2018; Novák et al. 2018). This complicates forensic analyses, as misidentification can lead to significant errors in minPMI estimations. Molecular tools such as Sanger sequencing have improved accuracy, but are time-consuming, costly, and destructive to specimens (Daniel et al. 2017).

Alternative approaches, such as chemical profiling of CHCs, offer promising non-destructive options. CHCs are lipophilic compounds embedded in the insect's epicuticle that play important roles in water retention, species identification, and communication, such as mate recognition (Lockey 1980, 1988; Howard and Blomquist 2005; Blomquist and Bagnères 2010). The CHC composition can vary with sex, age, reproductive status, and environmental conditions, making them suitable candidates for chemotaxonomic and developmental markers (Page et al. 1997; Lockey 1992).

The forensic potential of CHC profiles has been demonstrated in dipterans, such as the blowflies *Lucilia sericata* (Meigen, 1826) and *Calliphora vicina* (Robineau-Desvoidy, 1830), where CHC composition has been successfully used to infer age and environmental exposure of empty puparia (Moore et al., 2017; Sharif et al., 2023a, 2023b, 2024). These findings have encouraged interest in

expanding similar approaches to other forensically relevant taxa. Despite this progress, comparable CHC-based analyses in coleopterans, especially across developmental stages, remain scarce, leaving a gap in understanding the potential of CHCs for beetle-based forensic applications.

Our study aims to bridge this gap by characterizing CHC profiles of *T. sinuatus* across its complete developmental cycle. We apply gas chromatography-mass spectrometry (GC-MS) for compound identification and quantify stage-wise and sex-specific variations. Furthermore, we evaluate the discriminatory power of CHC profiles using principal component analysis (PCA) and a random forest model.

This study has two primary goals: (1) to assess whether CHC profiles differ significantly across life stages and between sexes of *T. sinuatus*, and (2) to determine whether these profiles can be used as reliable markers for developmental stage classification in a forensic context. Our work provides foundational data for future efforts to develop non-invasive chemical tools for forensic beetle identification and aging.

METHODS AND MATERIALS

Insect Material and Rearing. A *T. sinuatus* culture was established by collecting adult beetles from a piece of rotten pork that had been used as bait in Rüsselsheim am Main (49.972702° N, 8.454279° E), Germany. Adult beetles were brought to the Institute of Legal Medicine in Frankfurt am Main, Germany, and placed inside a plastic box (measuring 11 x 7.75 x 7 inches) at room temperature (20°C ± 2). Adult beetles were provided with a small piece of pork as food and damp soil as a substrate. Eggs were deposited mainly in the damp soil adjacent to the pork and were collected from the soil for rearing. Eggs were collected and transferred to plastic Petri dishes containing ad libitum food and damp soil as a pupation medium. The Petri dishes, providing enough space for the larvae to move, were closed using elastic bands. They turned onto their sides, providing a narrow arrangement that allowed for monitoring the larval feeding and pupal chamber**.** All developmental stages of the beetles were identified as described by Jakubec et al. (2019), periodically sampled and stored at -18°C until analysis.

CHC Extraction and Sample Size

The number of individuals included in each extraction differed among developmental stages because CHC yield is strongly dependent on specimen size. Early instars of *T. sinuatus* are

extremely small and produce very low quantities of hydrocarbons; therefore, several individuals were pooled to obtain sufficient extract for reliable GC–MS detection (five individuals for first instars; three individuals for second and third instars). In contrast, single pupae and adult beetles have much larger surface areas and produce adequate CHCs for analysis, so one specimen per extraction was used.

All samples were placed in separate 2 mL headspace vials containing 500 µL of *n*-Hexane and sonicated for 10 minutes. The solvent extract was transferred to a clean autosampler vial and evaporated to dryness under a gentle stream of nitrogen. The dried residues were stored at room temperature until GC-MS analysis. Immediately before analysis, each sample was reconstituted in 100 µL of *n*-hexane, vortexed for 30 seconds, and a 1 µL aliquot was injected using the autosampler. A hexane blank was run after each injection to monitor carryover.

Chemical Analysis. The chemical analysis of all the extracts was conducted using an Agilent Technologies 6890 N Network GC with a split/splitless injector set at 250°C, connected to an Agilent 5973 Network Mass Selective Detector, and a Restek Rxi-1MS nonpolar capillary column (30 m × 0.25 mm ID, 0.25 µm film thickness). The elution process was carried out using helium at a rate of 1 mL/min. The oven temperature was programmed to remain at 50°C for 2 minutes before being ramped to 200°C at 25°C/min, then from 200°C to 260°C at 3°C/min, and finally from 260°C to 320°C at 20°C/min, where it was held for 2 minutes. GC data acquisition and processing were performed using Agilent ChemStation software. The mass spectrometer was operated in Electron Ionisation mode at 70 eV, and the scan range was set from 40–500 amu at 1.5 scans s^{-1}. The hydrocarbons were identified using a library search (NIST08), along with diagnostic fragmented ions and Retention index (RI). Retention indices were calculated using C23 to C29 *n*-alkanes present in the sample. No *n*-alkanes greater than C29 were present in the sample, and a retention index standard was not available at the time of measurement. Therefore, retention indices could not be calculated for the late-eluting compounds. Assuming that the compound assignments are correct for several late-eluting compounds that have entries in the NIST GC Retention Index Search Program (Build May 24, 2011), we could estimate the retention indices for the remaining compounds. Using the SRS1 cubic spline add-on for Excel (https://www.srs1software.com/), a cubic spline fit was created using the measured retention times as the x-values and the averaged retention indices from the NIST RI database for the compounds highlighted in bold in the table

below as the y-values. The curve fit was used to estimate (interpolate) the retention indices for the remaining compounds from their measured retention times. To assess the accuracy of the fit, the estimated retention indices for the two compounds that are not highlighted in bold were compared to the averaged retention indices for these compounds from the NIST RI database. Good agreement between the estimated retention indices and the averaged database values lends support to the compound assignments and suggests that the estimated retention indices for other late-eluting compounds are not unreasonable.

Compound	**RT (min)**	**NIST RI**	**Calculated RI**
11-MeC29	29.776	**2933**	
5,17DiMeC29	30.207	2976	2977
11-MeC31	31.313	**3132**	
11,17DiMeC31	31.465	3164	3160
5, 13DiMeC31	31.61	**3187**	
13+15MeC33	32.691	**3330**	

Retention indices highlighted in bold were used for the cubic spline fit.

CHC abbreviations used in this study follow IUPAC structural nomenclature: “C” denotes carbon chain length, integers indicate methyl-branching positions, and “Me,” “DiMe,” and “TriMe” indicate one, two, and three methyl groups, respectively. Where branching positions could not be determined unequivocally due to co-elution or similar mass spectral behavior, unresolved positions are represented using placeholder variables (x, y).

Statistical Analysis. Each extraction was treated as one independent biological replicate. During the analysis, each sample's peak area with the highest intensity was standardized to 100% to maintain consistency. To achieve uniformity, the peak areas of selected compounds in each sample were normalized relative to the total sum of all peak areas. To assess the normal distribution of the data, the *Shapiro-Wilk normality test* was conducted at a significance level of 0.05. The results indicated a departure from normal distribution. Consequently, the non-parametric *Kruskal-Wallis*

test was employed to examine differences in hydrocarbon percentages across different life stages, followed by *Dunn's test* with Bonferroni correction. A heat map was generated to represent compounds significantly contributing to visual variations between life stages and to observe patterns in the overall CHC composition. All analyses and visualizations were performed in RStudio (version 2025.05.1 “Mariposa Orchid”; RStudio, Windows) using R (version 4.5.2).

For a comprehensive exploration of CHC profiles, PCA was performed on centered and scaled CHC datasets using the prcomp() function in R. A static 3D PCA plot was generated with the plot3D package to visualize separation of developmental stages and sexes along the first three principal components, with axes labeled by the percentage of explained variance. In addition, biplots were constructed using the factoextra package (fviz_pca_biplot), which simultaneously displayed individual scores and variable loadings. Confidence ellipses were added to indicate group clustering, and arrows representing variables were scaled according to their contribution to the principal components. Boxplots were generated in R to illustrate the relative abundance of the key CHC compounds selected from the PCA biplot across developmental stages. Plots were created using the ggplot2 package in R Studio.

To assess whether CHC profiles could accurately predict developmental stages, we implemented Random Forest (RF) classification using the randomForest package in RStudio. The dataset included 27 samples characterized by 56 CHCs, representing six developmental stages (1st instar, 2nd instar, 3rd instar, pupa, female adult, and male adult).

An initial RF model was trained on the full dataset with 500 trees (ntree = 500) and 10 predictors randomly sampled at each split (mtry = 10). This approach provided a baseline estimate of classification performance across all available data. To evaluate the robustness of this result and to check for potential overfitting, we also examined the model’s built-in out-of-bag (OOB) error, which serves as an internal cross-validation procedure. For each sample, predictions were obtained from trees where the sample was not included in the bootstrap training set, thereby generating an independent error estimate. Both the full-model accuracy and the OOB error/confusion matrix were reported, with the latter visualized as a colored heatmap to aid interpretation of classification performance across developmental stages.

To identify the most informative predictors, we extracted variable importance measures from the Random Forest model. Two complementary metrics were considered: Mean Decrease Accuracy

(MDA) and Mean Decrease Gini (MDG). MDA estimates the loss in predictive accuracy when the values of a given compound are permuted, thereby highlighting variables essential for classification performance. MDG, by contrast, quantifies the average reduction in node impurity (Gini index) when a variable is used for splitting, thus reflecting its overall contribution to tree construction. Together, these measures provided insights into which CHCs most strongly influenced stage classification, offering both a direct assessment of their predictive power (MDA) and their structural role in model decisions (MDG).

RESULTS

A total of 56 CHCs were detected across all samples, but their number and identity varied strongly among developmental stages and between sexes (Table 1). Representative TICs and mass spectra supporting compound identification are provided in Supplementary Information.

First instar carried 16 CHCs, the second instar 15, the third instar 15, the pupa 32, adult males 46, and adult females 40. Thus, CHC richness was lowest in early larvae and highest in adults, with pupae representing an intermediate but clearly more complex profile than any larval instar. Most compounds were branched alkanes (mono-, di-, or trimethyl), while *n*-alkanes and a few alkenes (C25 alkene, C27 alkene, C29 alkene, C31 alkene) were also present. Branched alkanes dominated the profiles at all stages.

Early larval instars showed relatively simple profiles dominated by shorter-chain hydrocarbons (Table 1). The 1st instar exhibited only 16 CHCs, with *n*-alkanes such as C23, C25, and C29, as well as a few branched compounds including 3-MeC25, 11+13-MeC27, 3-MeC27, 13+15-MeC29, 13,15-DiMeC29, 13+15-MeC31, 13,17-DiMeC31, 15+17-MeC33, and x,13-DiMeC33. The 2nd instar added a small number of additional CHCs (total 15), notably C26, 7-MeC25, and higher relative amounts of 3-MeC25 and 3-MeC27, while still lacking most of the long-chain dimethyl and trimethyl compounds found later. The 3rd instar also carried 15 CHCs but with a shift in relative abundance: 3-MeC25 peaked in the 3rd instar, and 3-MeC27 and 13+15-MeC31 reached their highest larval proportions, indicating the onset of more branched and longer-chain CHCs towards the end of larval development.

The pupal stage showed a clear step change in composition and richness, with 32 CHCs detected. Several CHCs were present in pupae but absent from all larval instars, including 11,15-DiMeC25,

5,9DiMeC25 & 5,x-DiMeC25, 5,x,y-TriMeC25, 16-MeC26 & 9,15-DiMeC26, 4-MeC26, 9-MeC27, 7-MeC27, 9,17-DiMeC27, 5+11-DiMeC27, 5,x,y-TriMeC27, 4,8,12-TriMeC28, 11+13-MeC29, 11+13-MeC31, y,13-DiMeC33, and others. Several compounds were essentially restricted to the pupal stage overall, such as 11,15-DiMeC25, 7-MeC27, and y,13-DiMeC33, which did not occur in any larval or adult samples. Common *n*-alkanes such as C23, C25, C27, C29, and C31 alkene were also present in pupae, but often at lower proportions than in larvae and adults.

Across all stages, a few CHCs were present in almost every sample, including C25, C27, 9+11-MeC25, C29, 13+15-MeC29, C31 alkene, 13+15-MeC31, and 15+17-MeC33, which formed a conserved "backbone" of the CHC profile. In contrast, certain compounds showed clear increasing or decreasing trends with development. For example, 3-MeC25 increased from the 1st to 3rd instar and remained abundant in pupae, but was undetected in both adults. C23 and C24 were mainly associated with larval and early stages, decreasing markedly in pupae and adults. Pupae and adults showed higher frequencies and abundances of long-chain dimethyl and trimethyl CHCs, such as TriMeC28, TriMeC29, TriMeC31, and multiple DiMeC29 and DiMeC31 isomers, which were absent from larvae.

Adult beetles exhibited the richest and most complex CHC profiles, with 46 CHCs detected in males and 40 in females. Most CHCs (36 compounds) were shared by both sexes but differed in relative abundance. A subset of CHCs occurred only in adult males (i.e., detected in males and absent in females): 9-MeC27, C28, 16-MeC28 & 8,14/16-DiMeC28, TriMeC28, 11,17/19-DiMeC31, 5,13/15-DiMeC31, 5,9,17-TriMeC31, and 13+15-MeC33. Some of these, such as C28, 16-MeC28 & 8,14/16-DiMeC28, and TriMeC28, were not detected at any earlier stage, indicating male-specific expression among adults.

Table 1 Cuticular hydrocarbon profile of *Thanatophilus sinuatus*, showing retention time (RT), compound identity (ID), Retention index (RI), and total percent area (mean ± SD) of each compound across developmental stages (first instar, second instar, third instar, pupa, adult male, and adult female; n as indicated). Dashes indicate absence of the compound in that stage. Chi-square (χ^2) values and associated p-values indicate statistical significance of variation in abundance among stages

RT	ID	CHC	RI	1st Instar n=5	2nd Instar n=5	3rd Instar n=5	Pupa n=5	Adult (Male) n=5	Adult (Female) n=2	χ^2	p-value
17.49	1	C23	2300	2.12±0.46	1.94±0.55	2.26±1.02	-	1.09±0.44	1.44±0.32	22.62	3.99E-04
19.43	2	C24	2400	-	-	0.96±0.45	-	0.86±0.29	1.04±0.09	25.39	1.17E-04
20.96	3	C25 Alkene	2426	-	-	-	-	0.86±0.06	8.31±0.61	25.72	1.01E-04
21.485	4	C25	2500	23.53±1.66	16.10±5.22	28.21±4.77	7.36±0.50	6.52±0.38	5.23±0.56	22.99	3.39E-04
22.257	5	9+11-MeC25	2538	1.25±0.24	3.10±1.25	1.61±0.73	6.83±0.76	4.25±0.71	3.74±0.59	24.03	2.14E-04
22.357	6	7-MeC25	2543	-	1.47±0.71	1.04±0.40	3.09±0.39	-	-	24.78	1.53E-04
22.862	7	11,15-DiMeC25[1]	2566	-	-	-	0.99±0.51	-	-	25.65	1.04E-04
22.985	8	7,11-DiMeC25[1]	2572	-	-	-	-	0.92±0.17	1.24±0.18	25.42	1.16E-04
23.019	9	3-MeC25	2574	1.51±0.41	5.80±2.32	7.13±2.35	6.36±0.73	-	-	24.39	1.83E-04
23.226	10	5,x-DiMeC25	2583	-	-	-	1.00±0.32	0.22±0.12	3.93±0.49	25.61	1.06E-04
23.593	11	C26	2600	-	1.19±0.40	1.86±0.59	3.13±0.65	4.13±0.38	1.09±0.14	24.22	1.97E-04
23.767	12	5, x, y-TriMeC25[1]	2608	-	-	-	3.31±0.74	0.67±0.21	3.20±1.43	25.33	1.21E-04
24.328	13	16-MeC26 & 9,15-DiMeC26[1,2]	2635	-	-	-	2.67±0.85	3.29±1.04	1.35±0.15	24.84	1.49E-04
24.838	14	4-MeC26	2659	-	-	-	2.49±0.39	-	4.08±3.46	25.25	1.25E-04
24.995	15	Mix DiMe C26[1]	2666	-	-	-	-	0.88±0.42	1.35±0.15	25.25	1.25E-04
25.209	16	C27 Alkene	2676	-	-	-	-	0.87±0.34	1.00±0.39	25.27	1.24E-04
25.733	17	C27	2700	12.39±2.06	13.40±2.11	14.41±4.16	6.31±2.01	7.76±0.27	0.68±0.01	23.59	2.61E-04

26.446	18	11+13-MeC27	2734	12.40±2.32	23.70±7.39	10.71±3.53	5.44±033	5.20±0.29	6.98±1.69	19.66	1.45E-03
26.531	19	9-MeC27	2738	-	-	-	4.25±0.98	4.11±0.26	-	24.73	1.57E-04
26.633	20	7-MeC27	2743	-	-	-	3.57±0.28	-	-	25.65	1.04E-04
26.808	21	3-MeC27	2751	1.06±0.35	2.83±0.99	2.10±0.68	4.90±036	-	2.47±1.44	24.65	1.63E-04
27.059	22	11,15-DiMeC27[1]	2762	-	-	-	-	3.04±0.51	6.01±0.10	25.72	1.01E-04
27.108	23	9,17-DiMeC27[1]	2765	-	-	-	2.85±0.66	2.298±1.01	5.15±1.36	23.69	2.49E-04
27.201	24	7,11-DiMeC27[1]	2769	-	-	-	-	2.30±0.48	-	25.65	1.04E-04
27.479	25	5+11-DiMeC27[1]	2781	-	-	-	1.60±0.27	1.63±0.38	3.97±1.25	24.15	2.03E-04
27.802	26	7, 11, 15-TriMeC27[1]	2796	-	-	-	-	1.72±0.34	2.61±0.47	25.27	1.24E-04
27.893	27	C28	2800	-	-	-	-	1.97±0.36	-	25.65	1.04E-04
28.037	28	5, x, y-TriMeC27[1]	2810	-	-	-	2.98±0.55	2.78±0.44	-	24.26	1.94E-04
28.564	29	16-MeC28 & 8,14/16-DiMeC28[1,2]	2845	-	-	-	-	3.80±0.76	-	25.65	1.04E-04
28.945	30	TriMeC28[1]	2870	-	-	-	-	2.92±0.54	-	25.65	1.04E-04
29.128	31	C29 Alkene	2882	-	-	-	-	-	0.70±0.37	20.66	9.39E-04
29.301	32	TriMeC28[1]	2893	-	-	-	-	0.89±0.19	0.49±0.03	25.65	1.04E-04
29.409	33	C29	2900	8.90±2.59	5.51±0.90	3.10±2.68	3.57±0.56	1.93±0.50	0.98±0.38	25.96	9.08E-05
29.6	34	4, 8, 12-TriMeC28[1]	2917	-	-	-	2.39±1.46	-	1.21±0.75	20.797	8.85E-04
29.742	35	13+15-MeC29	2930	7.30±1.35	6.77±2.33	3.35±1.66	2.21±0.15	2.07±0.44	2.15±0.79	17.09	4.33E-03
29.776	36	11+13-MeC29	2933	-	-	-	3.51±0.49	2.45±0.08	1.32±0.50	25.61	1.06E-04

29.994	37	13,15-DiMeC29[1]	2954	1.66±0.68	-	-	2.72±1.20	1.29±0.10	3.79±0.47	24.85	1.49E-04
30.041	38	11,17-DiMeC29[1]	2959	-	-	-	-	3.30±0.64	2.60±0.56	25.72	1.01E-04
30.207	39	5,17-DiMeC29[1]	2977	-	-	-	-	1.10±0.04	3.59±0.89	25.72	1.01E-04
30.415	40	5,9,15-TriMeC29[1]	3000	-	-	-	-	2.38±0.26	2.36±1.35	25.42	1.16E-04
30.614	41	3,9,15-TriMeC29[1]	3025	-	-	-	-	2.39±0.35	2.14±0.85	25.72	1.01E-04
30.789	42	14,18-DiMeC30[1]	3048	-	-	-	-	-	-	-	-
31.088	43	C31 Alkene	3093	2.54±1.39	1.33±0.56	1.53±0.50	1.52±0.80	1.43±0.41	1.07±0.38	21.8	5.71E-04
31.267	44	13+15-MeC31	3124	11.63±2.03	11.79±2.43	16.43±5.37	1.80±0.39	1.07±0.03	1.62±1.13	20.46	1.02E-03
31.313	45	11+13-MeC31	3132	-	-	-	4.28±1.99	1.95±0.09	1.64±0.24	25.61	1.06E-04
31.437	46	13,17-DiMeC31[1]	3155	3.30±1.02	-	-	1.94±0.91	1.03±0.06	1.87±0.98	24.58	1.68E-04
31.465	47	11,17/19-DiMeC31[1]	3160	-	-	-	-	1.18±0.12	-	25.65	1.04E-04
31.533	48	7,11/19-DiMeC31[1]	3173	-	-	-	-	1.26±0.16	1.61±0.48	25.27	1.24E-04
31.61	49	5, 13/15-DiMeC31[1]	3187	-	-	-	-	1.48±0.11	-	25.65	1.04E-04
31.783	50	5, 9, 17-TriMeC31[1]	3216	-	-	-	-	2.26±0.51	-	25.65	1.04E-04
31.932	51	16+18-MeC32	3238	1.74±0.81	0.75±0.14	-	1.59±0.45	1.32±0.76	0.94±0.05	23.64	2.54E-04
31.981	52	8,15-DiMeC32[1]	3245	-	-	-	-	1.58±0.86	2.27±0.30	25.27	1.24E-04
32.639	53	15+17-MeC33	3324	4.58±0.80	4.34±2.17	5.30±2.20	1.43±0.36	0.99±0.23	1.53±0.67	12.06	3.39E-02
32.691	54	13+15-MeC33	3330	-	-	-	1.95±0.71	1.79±0.26	-	24.36	1.85E-04
32.814	55	x,13-DiMeC33[1]	3344	4.08±0.70	-	-	1.07±0.13	0.81±0.04	1.27±0.23	23.97	2.20E-04
32.887	56	y,13-DiMeC33[1]	3352	-	-	-	0.90±0.13	-	-	25.65	1.04E-04

[1]Tentative identification based on Retention Index values match with NIST08 Library database

[2]Co-eluting peaks

Adult females, in turn, showed four CHCs not detected in males: 7,11-DiMeC25, 4-MeC26, C29 alkene, and 4,8,12-TriMeC28. A few compounds were present in both sexes but clearly differed in abundance; for example, 3-MeC27 occurred in larvae, pupae, and females but was absent in adult males, whereas several long-chain di- and trimethyl C29–C31 compounds (e.g., 11,17-DiMeC29, 5,17-DiMeC29, 5,9,15-TriMeC29, 3,9,15-TriMeC29) were shared but tended to be more prominent in males. Overall, adult males carried more unique long-chain, highly branched CHCs, whereas females combined these with female-exclusive compounds and substantial contributions from 3-MeC25 and 3-MeC27 that also occurred in immature stages.

The heatmap of all 56 CHCs (Fig. 1) visualized these patterns, with lighter colours in larval instars and progressively more intense and numerous signals in pupae and adults. Larval stages shared broadly similar profiles dominated by a modest set of short- to mid-chain CHCs, while pupae showed a wider range of CHCs, and adults, particularly males, exhibited the highest overall signal density. Adult females also formed a distinct band in the heatmap, reflecting their combination of shared and female-exclusive compounds.

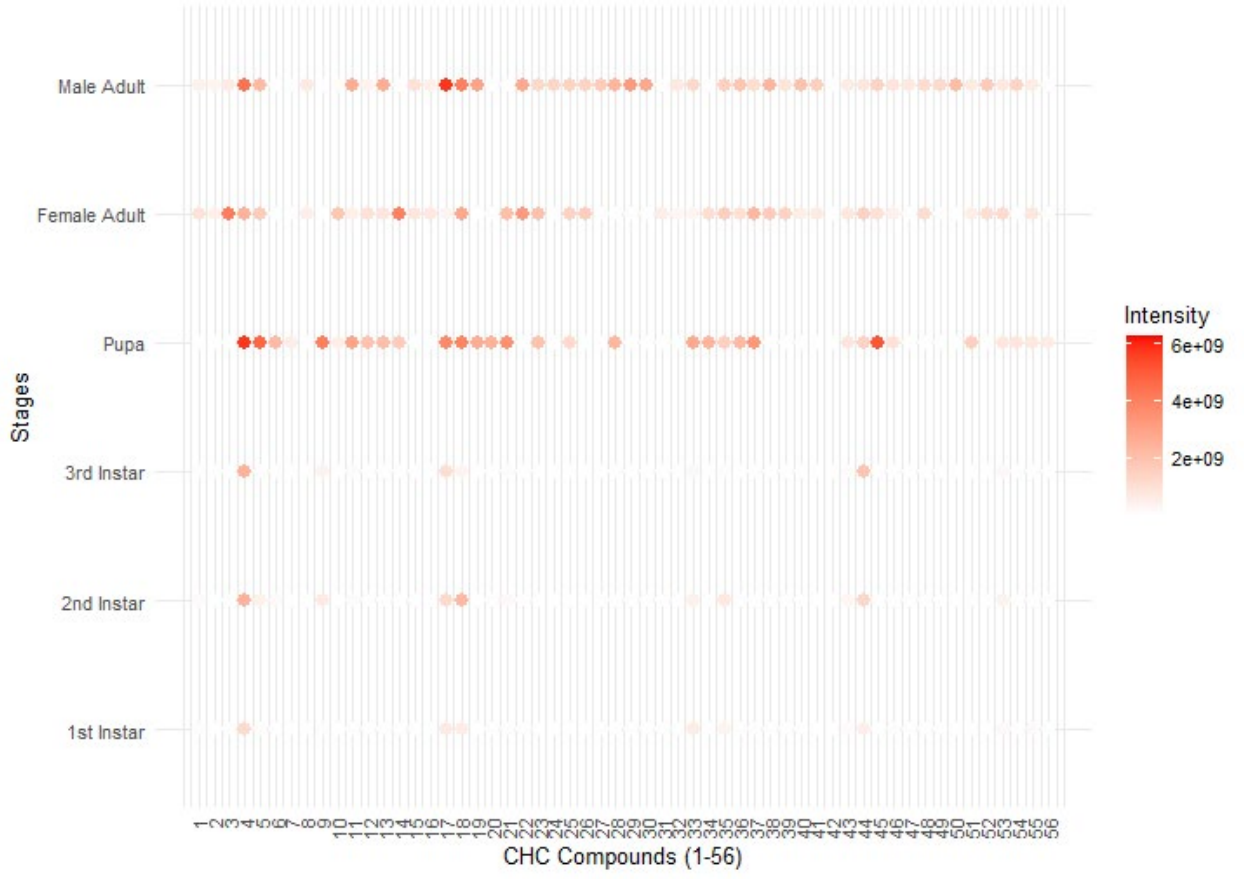


Fig. 1 Heatmap of 56 CHC compounds across developmental stages of the *Thanatophilus sinuatus*. The X-axis shows CHC number (1–56), the y-axis shows stages from 1st Instar to Male Adult. Dot color intensity (white to red) indicates CHC abundance

Further PCA (Fig. 2) showed clear separation among life stages. The first three principal components explained 86.7% of the total variance. Larval instars clustered tightly, indicating broadly similar CHC compositions in early development. Pupae formed a separate cluster, driven by their richer set of C27-based and longer-chain methyl-branched compounds (e.g., 11+13-MeC27, 3-MeC27, 7-MeC27, 5,x,y-TriMeC25, and related di- and trimethyl CHCs). Adult males and females clustered together in PCA space but were clearly separated from both larvae and pupae, reflecting their more complex and branched CHC profiles.

The PCA biplot (Fig. 3) identified a subset of CHCs contributing most strongly to stage separation, including 3-MeC25, 3-MeC27, 7-MeC25, 7,11-DiMeC25, 11,15-DiMeC25, 5,x,y-TriMeC25, 11+13-MeC29, several di- and trimethyl C29 and C31 compounds (e.g., 11,17-DiMeC29, 3,9,15-TriMeC29, TriMeC28, 5,9,15-TriMeC29), and y,13-DiMeC33. These compounds showed clear stage-biased or sex-biased distributions in Table 1 and in the univariate plots.

Barplots (Fig. 4) and boxplots (Fig. 5) of these key CHCs confirmed that larval instars were characterised by higher relative abundances of 3-MeC25, C23, C25, and C29, whereas pupae were distinguished by strong contributions from 11+13-MeC27, 3-MeC27, 7-MeC25, 5,x,y-TriMeC25, and several C27 dimethyl and trimethyl compounds. Adult stages showed the highest variability and abundance across long-chain di- and trimethyl CHCs, with some compounds enriched in males and others more pronounced in females, consistent with the sex-specific patterns described above.

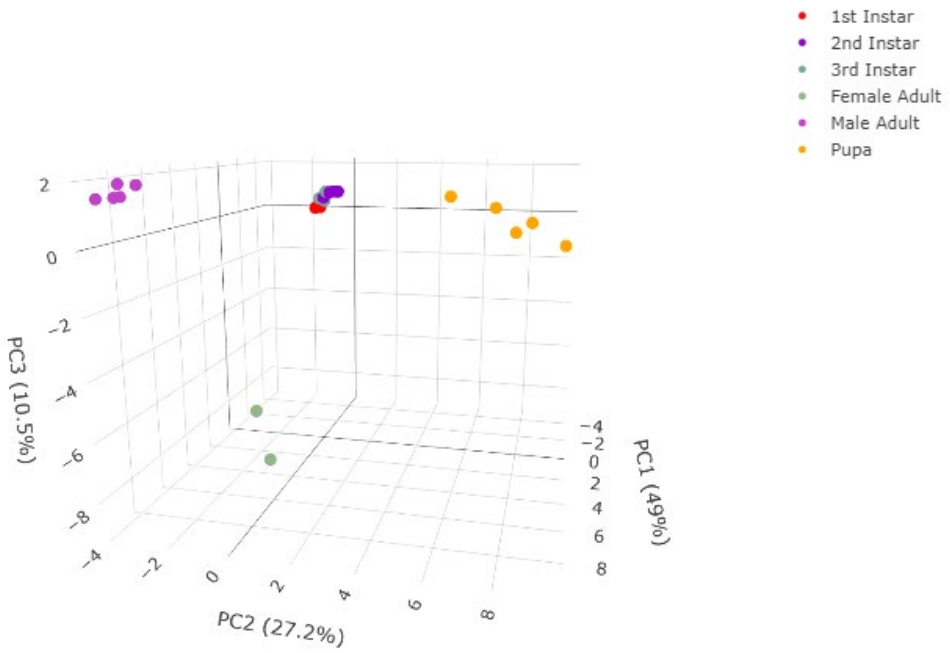


Fig. 2 Three-dimensional PCA plot illustrating the differentiation of life stages in *Thanatophilus sinuatus* based on CHC profiles. The first three principal components, which collectively account for 86.7% of the total variance, are shown on the x-, y-, and z-axes. Each point represents an individual sample, with colours (and/or symbols) indicating developmental stages (1st instar, 2nd instar, 3rd instar, pupa, adult male, and adult female). The clear separation of clusters reflects distinct CHC compositions among larval, pupal, and adult stages.

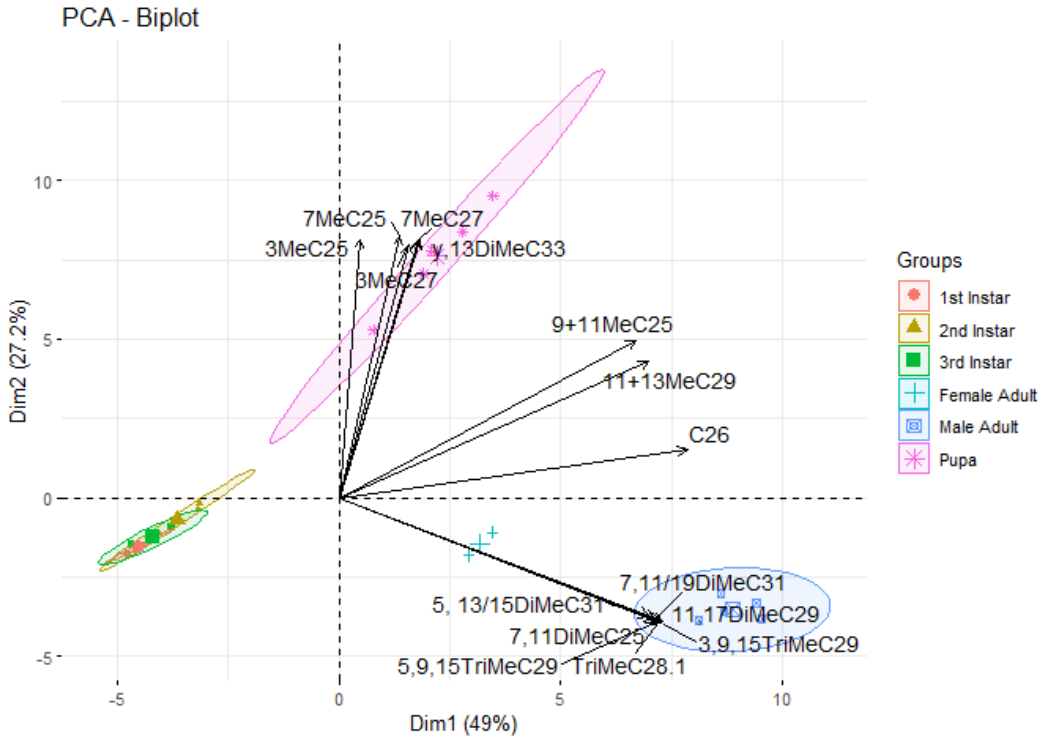


Fig. 3 PCA biplot showing the variation in CHC profiles across developmental stages of the *T sinuatus*. Dim1 (49%) and Dim2 (27.2%) explain the major variation in the dataset. Arrows represent individual CHC compounds, and their direction and length indicate contribution to the separation of stages. Ellipses highlight the 95% confidence intervals for each stage, illustrating stage-specific clustering

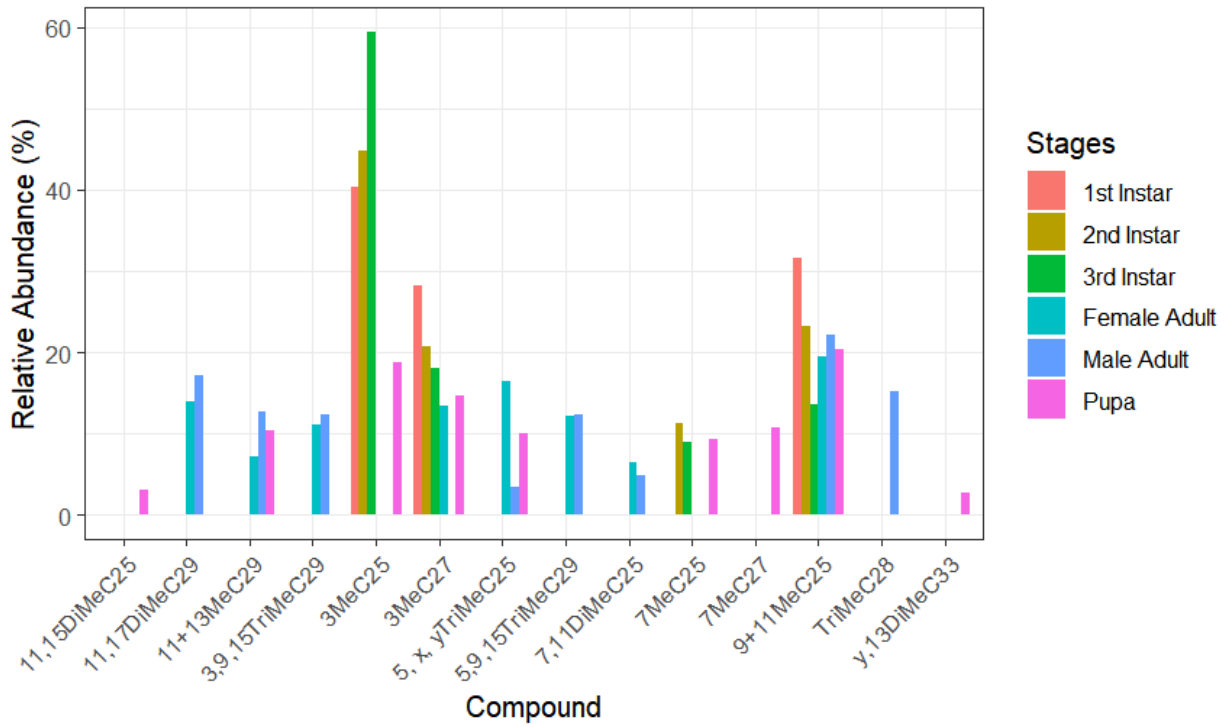


Fig. 4 The barplots depict the key CHCs extracted from the biplot, highlighting the compounds that display the most robust associations and variability with each life stage. This visual representation offers a detailed insight into the relative abundance and distribution patterns of these key compounds across different developmental classes of *T. sinuatus*. Each bar represents the mean relative abundance (%) of individual compounds at different stages. Compounds are labeled along the x-axis. Differences in relative abundance highlight stage-specific CHC profiles

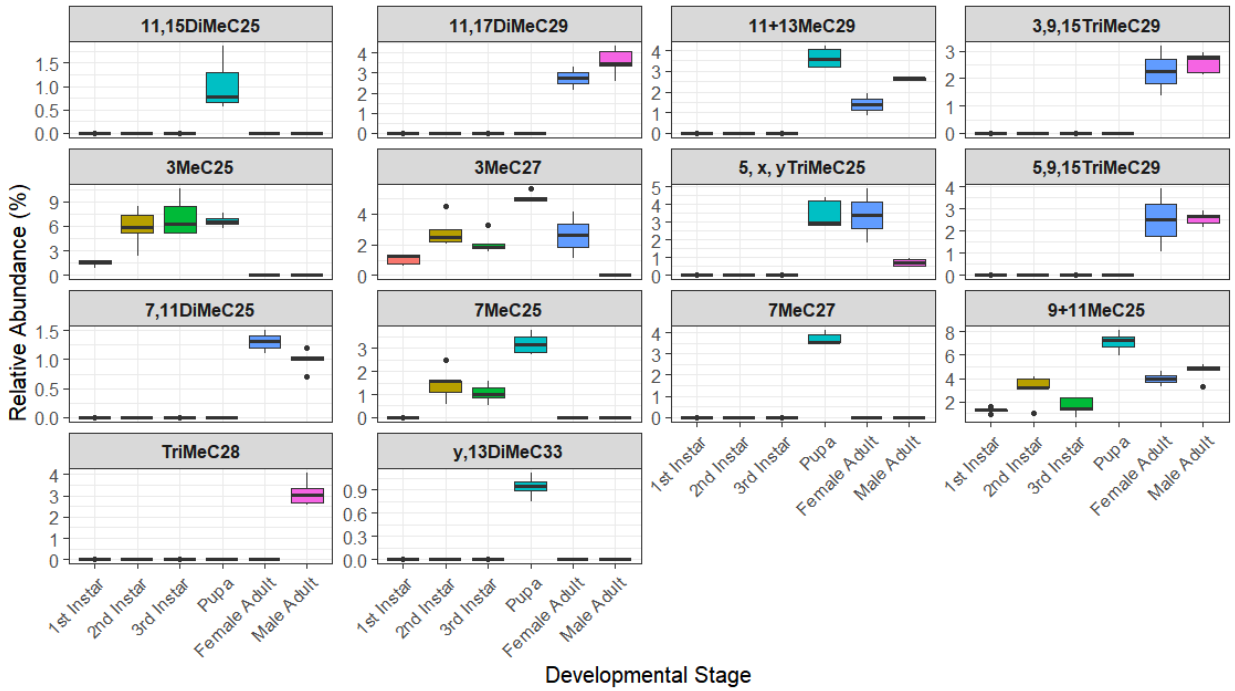


Fig. 5 Boxplots showing the relative abundance of key CHCs associated with developmental stages of *T. sinuatus*, as indicated by the PCA biplot. Each box represents the interquartile range, the horizontal line shows the median, and whiskers depict the minimum and maximum values, highlighting stage-specific CHC variation

Further, Random Forest classification using 56 CHCs achieved 100% accuracy in predicting developmental stages across the dataset, with all six stages (1st instar, 2nd instar, 3rd instar, pupa, female adult, and male adult) being correctly classified. To ensure this result was not due to overfitting, model performance was further validated using the OOB error estimate. The OOB error rate was 3.7%, still reflecting very high predictive accuracy. The colored OOB confusion matrix (Fig. 6) confirmed perfect classification for 1st instar, 2nd instar, 3rd instar, pupa, and male adult, with a single misclassification observed between female and male adults.

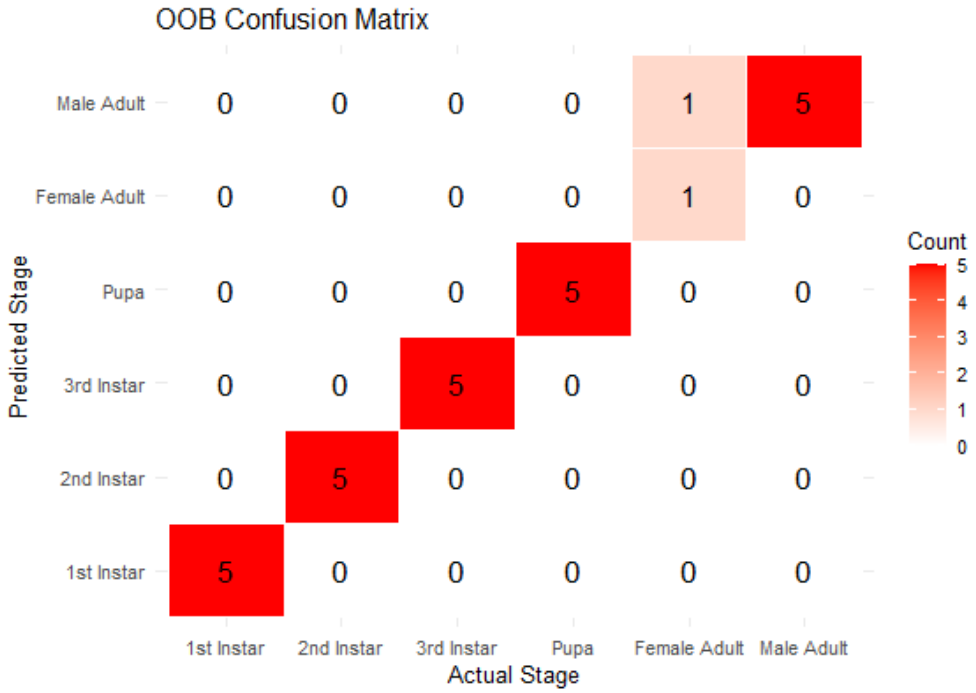


Fig. 6 Out-of-bag confusion matrix of Random Forest classification. The matrix compares predicted versus actual developmental stages based on CHC profiles. High accuracy was observed across most stages, with minor misclassification in the Female Adult category, likely due to limited sample size. The OOB error rate (3.7%) provides an unbiased internal estimate of model performance

Further, Random Forest classification using all 56 CHCs achieved 100% apparent accuracy on the full dataset and an OOB error rate of 3.7%, indicating very high predictive power of CHC profiles for developmental stage classification. The OOB confusion matrix (Fig. 6) showed perfect classification for 1st instar, 2nd instar, 3rd instar, pupae, and adult males, with a single misclassification between female and male adults, likely reflecting both the small number of female samples and their partial overlap with male CHC space. The MDA values showed that removing key CHCs such as C29, C25, 16+18-MeC32, 7-MeC25, 9+11-MeC25, C31 alkene, 3-

MeC27, 13,15-DiMeC29, 11+13-MeC27, and 13+15-MeC31 caused the largest reduction in model accuracy, confirming their high predictive influence (Fig. 7). MDG values similarly highlighted these CHCs as important contributors to decision splits within the trees, reinforcing their strong role in distinguishing stages. CHCs ranked highly by both MDA and MDG correspond to compounds that show clear developmental structuring across larvae, pupae, and adults.

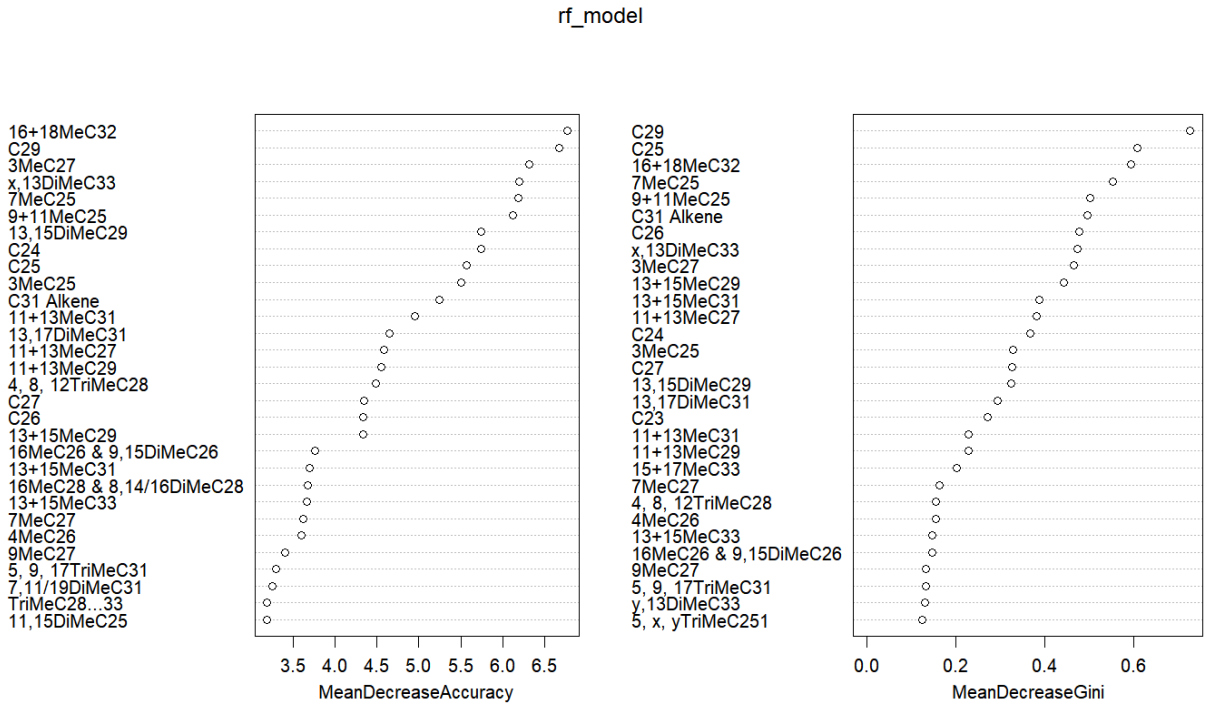


Fig. 7 Variable-importance plot from the Random Forest model for developmental stage classification in *T. sinuatus*. The graph shows the CHCs with the highest contribution to classification performance, measured by Mean Decrease Accuracy (left) and Mean Decrease Gini (right). Compounds including C29, C25, 16+18-MeC32, 7-MeC25, 9+11-MeC25, C31 alkene, 3-MeC27, 13,15-DiMeC29, 11+13-MeC27, and 13+15-MeC31 were the most informative predictors, reflecting strong developmental structuring across stages.

DISCUSSION

The successful chemical differentiation of all life stages of *T sinuatus* using CHC profiles validates their potential as robust biomarkers for species identification and age estimation in forensic entomology. The highly distinct chemical profiles, confirmed by multivariate statistical analyses (PCA) and high-accuracy classification models (Random Forest), confirm that CHC profiling provides a non-destructive, complementary tool to traditional morphological identification. Although the larval instars of this species can be separated morphologically using published keys (Jakubec et al. 2019), the chemical composition of the cuticle provides an additional, objective

marker of stage. Such chemical data become valuable when specimens are damaged, incomplete, or present only as traces, situations in which external structures normally used for identification (e.g., size or head-capsule features) may be missing or obscured. The ability to differentiate between developmental stages based on CHC composition could improve the accuracy of insect-based estimates of time of death in forensic investigations. It is also imaginable that, within a developmental stage (e.g., the third larval stage, which can last several days depending on the ambient temperature), a more precise analysis with day-specific resolution is possible with the help of CHC analysis. Currently, we only know when a stage is reached and how long it lasts (Montoya-Molina et al. 2021; Shao et al. 2025). However, further research is necessary to fully understand the utility of CHCs as forensic markers in *T. sinuatus* and other insects.

The ontogenetic shift in CHC composition we observed for *T sinuatus*, a relative enrichment of longer-chain *n*-alkanes and methyl-branched components in later developmental stages, matches patterns reported in other beetles. Although direct CHC profiles for most *Thanatophilus* species are not available, studies on other Staphylinid beetles show stage-dependent changes in cuticular chemistry consistent with ours. In the burying beetle *Nicrophorus vespilloides* (Herbst, 1783), for example, cuticular and volatile profiles change markedly across larval instars and into adulthood, with adults displaying more complex and longer-chain compounds (Sahm et al. 2024; Steiger et al. 2007). These congruent patterns indicate that the developmental CHC trajectory we report for *T. sinuatus* likely reflects conserved physiological maturation of the epicuticular lipid layer and the emergence of adult functions such as desiccation resistance and chemical communication. However, direct comparisons between *Thanatophilus* species remain limited in the literature, highlighting the need for expanded CHC characterization within this genus.

Beyond developmental relevance, the species-level specificity of CHC mixtures underlines their strong chemotaxonomic utility in Coleoptera. For example, a CHC-based chemotaxonomic study of five species from three genera of Gonipterini weevils (Curculionidae) successfully discriminated all taxa based on their cuticular profiles (Johnson 2022). Among scarab beetles, a recent analysis of six species of scarabid beetle *Cyclocephala* (Dejean, 1821) identified 74 cuticular compounds; a subset of ten hydrocarbons accounted for over 85 % of inter-species dissimilarity (Santos et al. 2024). Studies in other insect groups have demonstrated clear distinctions in CHC profiles between life stages and sexes (Finck et al. 2016; Vernier et al. 2019;

Sprenger and Menzel 2020). These findings indicate that qualitative differences in chain lengths, branching patterns, and compound suites are robust chemotaxonomic markers. In this light, the CHC profile we report for *T. sinuatus* likely represents a species- and stage-specific chemical fingerprint, and provides a valuable baseline for future comparative and forensic studies.

Furthermore, literature shows that diet, substrate, and environmental stressors (temperature, humidity/desiccation) can change CHC composition qualitatively and quantitatively. Experimental studies in beetles and other insects have revealed that the distribution of CHC chain lengths and their relative abundances respond plastically to desiccation regimes and dietary differences (Botella-Cruz et al. 2017, 2021; Claudio-Piedras et al. 2021). For example, saline-habitat beetles adjust CHC composition under desiccation to reduce water loss, and diet-manipulation studies in insects commonly report shifts in specific CHC components. We reared our specimens under standardized laboratory conditions to limit such variation, but residual diet/substrate or microenvironmental differences could contribute to within-stage variability; therefore, interpretation of subtle abundance shifts should explicitly acknowledge these possible influences.

Positioning *T. sinuatus* CHC ontogeny within coleopteran patterns validates the potential of CHC profiling for developmental stage discrimination in forensic contexts, especially when morphological characters are absent. Because dedicated CHC datasets in this family remain limited, our data provide useful baseline profiles for *T. sinuatus* and motivate additional comparative CHC work across burial/carrion beetle congeners and populations under controlled diet and microclimate regimes. Integrating such family-level comparative data will increase confidence in CHC-based forensic markers and allow quantification of environmental variance important for casework.

CONCLUSION

This study demonstrates that CHC profiles vary significantly across the developmental stages and sexes of *T sinuatus*, with clear qualitative and quantitative shifts observable from early larvae to adults. Larval stages were characterized by simpler profiles dominated by short- to mid-chain hydrocarbons, whereas pupae and adults showed increased diversity and higher proportions of longer-chain, methyl-branched compounds. These chemical differences were supported by multivariate analyses, with PCA clearly separating stages and Random Forest classification achieving very high prediction accuracy, including successful discrimination of all larval instars

and pupae. The stage-specific and sex-associated CHC signatures identified here support the application of CHC profiling as a complementary tool for developmental stage identification of *T. sinuatus*, particularly in forensic situations where morphological features are damaged or incomplete. Our findings provide a foundational dataset for this forensically important species and highlight the value of CHCs as reliable chemical markers for improving post-mortem interval estimation.

LIMITATIONS AND FUTURE DIRECTIONS

We acknowledge a limitation of our study in that we only analyzed CHCs from a single population of *T. sinuatus*. Populations from different geographic locations may have different CHC compositions (Byrne et al. 1995; Hadley 1978; Howard and Blomquist 2005), which may affect the conclusions drawn from our study. Future research should aim to sample multiple populations of *T. sinuatus* and other insect species to determine the generalizability of our results. Another limitation of this study was the relatively small number of female specimens, which likely explains the reduced classification accuracy in this group rather than a systematic overlap in CHC profiles. Increasing the representation of female samples in future studies would help refine sex specific predictions, but this does not diminish the overall robustness of developmental stage classification achieved here. Instead, our findings highlight the potential of CHC-based approaches as reliable complementary tools in forensic entomology, particularly when supported by machine learning algorithms. The CHCs highlighted by the variable importance analysis may serve as candidate biomarkers for developmental stage classification. These compounds, if validated across larger and more diverse datasets, could provide robust chemical markers for forensic applications. Future studies incorporating quantitative profiling of these key CHCs, along with expanded sample sizes, will strengthen their reliability and generalizability. In addition, integrating these biomarkers into advanced machine learning frameworks may further enhance postmortem interval estimation and broaden the applicability of CHC-based forensic entomology.

Funding:

Scientific Exchange Grant (9040) was awarded to Swaima Sharif by the European Molecular Biology Organization (EMBO) to conduct this work.

REFERENCES:

Amendt J, Richards CS, Campobasso CP, Zehner R, Hall MJ (2011) Forensic entomology: applications and limitations. Forensic Sci Med Pathol 7:379–392. https://doi.org/10.1007/s12024-010-9209-2

Blomquist G, Bagnères A (2010) Insect hydrocarbons: biology, biochemistry, and chemical ecology. Cambridge University Press. https://doi.org/10.1017/CBO9780511711909

Botella-Cruz M, Velasco J, Millán A, Hetz S, Pallarés S (2021) Cuticle Hydrocarbons Show Plastic Variation under Desiccation in Saline Aquatic Beetles. Insects 12(4): 285. https://doi.org/10.3390/insects12040285

Botella-Cruz M, Villastrigo A, Pallarés S, López-Gallego E, Millán A, Velasco J (2017) Cuticle hydrocarbons in saline aquatic beetles. PeerJ, 5, e3562. https://doi.org/10.7717/peerj.3562

Byrne AL, Camann MA, Cyr TL, Catts EP, Espelie KE (1995) Forensic Implications of Biochemical Differences Among Geographic Populations of the Black Blow Fly, Phormia regina (Meigen). J Forensic Sci 40(3):13789J. https://doi.org/10.1520/JFS13789J

Claudio-Piedras F, Recio-Tótoro B, Cime-Castillo J, Condé R, Maffei M (2021) Dietary and Plasmodium challenge effects on the cuticular hydrocarbon profile of Anopheles albimanus. Sci Rep 11, 11258. https://doi.org/10.1038/s41598-021-90673-x

Daniel CA, Midgley JM, Villet MH (2017) Determination of species and instars of the larvae of the Afrotropical species of Thanatophilus Leach, 1817 (Coleoptera, Silphidae). Afr Invertebr 58(2):1-10, 58(2):1–10. https://doi.org/10.3897/AFRINVERTEBR.58.12966

Dekeirsschieter J, Verheggen FJ, Haubruge E, Brostaux Y (2011) Carrion beetles visiting pig carcasses during early spring in urban, forest and agricultural biotopes of Western Europe. J Inst Sci 11:1–13. https://doi.org/10.1673/031.011.7301

Finck J, Berdan EL, Mayer F, Ronacher B, Geiselhardt S (2016) Divergence of cuticular hydrocarbons in two sympatric grasshopper species and the evolution of fatty acid synthases and elongases across insects. Sci Rep 6(1):1–13. https://doi.org/10.1038/srep33695

Frątczak-Łagiewska K, Matuszewski S (2018) Sex-specific developmental models for Creophilus maxillosus (L.) (Coleoptera: Staphylinidae): searching for larger accuracy of insect age estimates. Int J Legal Med 132:887–895. https://doi.org/10.1007/s00414-017-1713-4

Hadley NF (1978) Cuticular permeability of desert tenebrionid beetles: Correlations with epicuticular hydrocarbon composition. Insect Biochem 8(1):17–22. https://doi.org/10.1016/0020-1790(78)90005-7

Howard RW, Blomquist GJ (2005) Ecological, behavioral, and biochemical aspects of insect hydrocarbons. Annu Rev Entomol 50:371–393. https://doi.org/10.1146/ANNUREV.ENTO.50.071803.130359

Jakubec P, Novák M, Qubaiová J, Šuláková H, Růžička J (2019) Description of immature stages of Thanatophilus sinuatus (Coleoptera: Silphidae). Int J Legal Med 133(5):1549–1565. https://doi.org/10.1007/s00414-019-02040-1

Johnson J B (2022) Cuticular Hydrocarbon Profiling Reveals Chemotaxonomic Diversity among *Gonipterini weevils* (Coleoptera: Curculionidae). Biol. Life Sci. Forum, 15(1):5. https://doi.org/10.3390/IECD2022-12383

Lockey K (1980) Insect cuticular hydrocarbons. Comp Biochem Physiol B: Biochem Mol Biol 65:457–462.

Lockey K (1988) Lipids of the insect cuticle: origin, composition, and function. Comp Biochem Physiol B: Biochem Mol Biol 89:595–645.

Lockey KH (1992) Insect hydrocarbon chemotaxonomy: Cuticular hydrocarbons of adult and larval Epiphysa species Blanchard and adult Onymacris unguicularis (Haag) (Tenebrionidae: Coleoptera). Comp Biochem Physiol Part B: Comp Biochem 102(3):451–470. https://doi.org/10.1016/0305-0491(92)90035-P

Lockey KH, Metcalfe NB (1988) Cuticular hydrocarbons of adult Himatismus species and a comparison with 21 other species of adult tenebrionid beetle using multivariate analysis. Comp Biochem Physiol Part B: Biochem Mol Biol 91(2):371–382. https://doi.org/10.1016/0305-0491(88)90156-3

Matuszewski S, Bajerlein D, Konwerski S, Szpila K (2008) An initial study of insect succession and carrion decomposition in various forest habitats of Central Europe. Forensic Sci Int 180:61–69. https://doi.org/10.1016/j.forsciint.2008.06.015

Midgley JM, Villet MH (2009) Development of Thanatophilus micans (Fabricius 1794) (Coleoptera: Silphidae) at constant temperatures. Int J Legal Med 123(4):285–292. https://doi.org/10.1007/s00414-008-0280-0

Montoya-Molina S, Jakubec P, Qubaiová J, Novák M, Šuláková H, Růžička J (2021) Developmental models of the forensically important carrion beetle, Thanatophilus sinuatus (Coleoptera: Silphidae). J Med Entomol 58(3):1041–1047. https://doi.org/10.1093/jme/tjaa255

Moore, H. E., Pechal, J. L., Benbow, M. E., & Drijfhout, F. P. (2017). The potential use of cuticular hydrocarbons and multivariate analysis to age empty puparial cases of Calliphora vicina and Lucilia sericata. Sci Rep, *7*(1), 1933. https://doi.org/10.1038/s41598-017-01667-7

Novák M, Jakubec P, Qubaiová J, Šuláková H, Růžička J (2018) Revisited larval morphology of Thanatophilus rugosus (Coleoptera: Silphidae). Int J Legal Med 132(3):939–954. https://doi.org/10.1007/S00414-017-1764-6

Page M, Nelson LJ, Blomquist GJ, Seybold SJ (1997) Cuticular hydrocarbons as chemotaxonomic characters of pine engraver beetles (Ips spp.) in the grandicollis subgeneric group. J Chem Ecol 23(4):1053–1099. https://doi.org/10.1023/B:JOEC.0000006388.92425.EC

Ratcliffe BC, Luedtke RJ (1969) A comparison of silphids taken from covered and uncovered

carrion (Coleoptera: Silphidae). Coleopt Bull 23:103–105

Ridgeway JA, Midgley JM, Collett IJ, Villet MH (2014) Advantages of using development models of the carrion beetles Thanatophilus micans (Fabricius) and T. mutilatus (Castelneau) (Coleoptera: Silphidae) for estimating minimum post mortem intervals, verified with case data. Int J Legal Med 128(1):207–220. https://doi.org/10.1007/S00414-013-0865-0

Sahm J, Brobeil B, Grubmüller E, Conrad T, Schott M, Stökl J, Steiger S (2024). The scent of offspring: Chemical profiles of larvae change during development and affect parental behavior in a burying beetle. Behav Ecol, *35*(5). https://doi.org/10.1093/beheco/arae061

Santos GKN, Navarro DM do AF, Maia ACD (2024) Cuticular lipid profiles of selected species of cyclocephaline beetles (Melolonthidae, Cyclocephalini). Bull. Entomol. Res, 114(1):124-133. https://doi.org/10.1017/S0007485323000664

Shao S, Hu G, Li L, Gao Y, Zhang R, Liu S, Xu H, Xia S, Wang Y (2025) Developmental time pattern of Thanatophilus sinuatus at different constant and variable temperatures. Forensic Sci Int 366:112301. https://doi.org/10.1016/j.forsciint.2024.112301

Sharif S, Wunder C, Kaleem Khan M, Amendt J, Qamar A (2023a) Degradation dynamics of cuticular hydrocarbons of empty puparia in Lucilia sericata in soil and under room conditions: insights and machine learning applications. Forensic Chem 35: 100519. https://doi.org/10.1016/j.forc.2023.100519

Sharif S, Wunder C, Khan MK, Qamar A, Amendt J (2023b) Cuticular hydrocarbons as weathering biomarkers of empty puparia of the forensically important blowfly Calliphora vicina Robineau-Desvoidy, 1830 (Diptera: Calliphoridae) in soil v/s under room conditions. Forensic Sci Int 349: 111748. https://doi.org/10.1016/j.forsciint.2023.111748

Sharif S, Wunder C, Amendt J, Qamar A (2024) Variations in cuticular hydrocarbons of Calliphora vicina (Diptera: Calliphoridae) empty puparia: insights for estimating late postmortem intervals. Int J Legal Med 138: 2717-2733. https://doi.org/10.1007/s00414-024-03296-y

Sprenger PP, Menzel F (2020) Cuticular hydrocarbons in ants (Hymenoptera: Formicidae) and other insects: how and why they differ among individuals, colonies, and species. Myrmecol News 30:1–26. https://doi.org/10.25849/myrmecol.news_030:001

Steiger S, Peschke K, Francke W, Müller JK (2007). The smell of parents: breeding status influences cuticular hydrocarbon pattern in the burying beetle Nicrophorus vespilloides. Proc Biol Sci. 274(1622). https://doi.org/10.1098/rspb.2007.0656

Vernier CL, Krupp JJ, Marcus K, Hefetz A, Levine JD, Ben-Shahar Y (2019) The cuticular hydrocarbon profiles of honey bee workers develop via a socially-modulated innate process. ELife 8. https://doi.org/10.7554/ELIFE.41855



https://dspace.org/

Cuticular hydrocarbons as biomarkers of developmental stages in Thanatophilus sinuatus (Fabricius, 1775) (Coleoptera: Staphylinidae): evidence from GC–MS and random forest modeling

Sharif, Swaima; Jakubec, Pavel; Moore, Hannah E.; Cody, Robert B.; Amendt, Jens ...

2026-06
Springer
https://doi.org/10.1007/s00114-026-02103-5
Sharif S, Jakubec P, Moore H, et al., (2026) Cuticular hydrocarbons as biomarkers of developmental stages in Thanatophilus sinuatus (Fabricius, 1775) (Coleoptera: Staphylinidae): evidence from GC–MS and random forest modeling. The Science of Nature, Volume 113, Issue 3, June 2026, Article number 52

Downloaded from a DSpace repository. https://dspace.org/